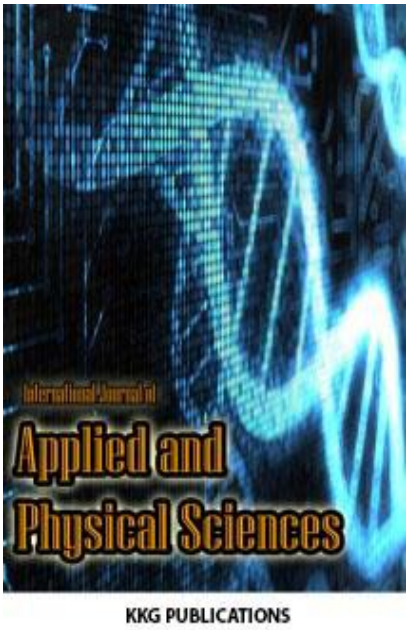

Key Knowledge Generation
Publication details, including instructions for authors and subscription information:
http://kkgpublications.com/applied-sciences/

Electrolyte Flow in an External Magnetic Field: A Dimensionless Analysis

LANKA DINUSHKE WEERASIRI [1], SUBRAT DAS [2]

[1, 2] Deakin University, Australia

Published online: 16 March 2016

To cite this article: L. D. Weerasiri and S. Das, "Electrolyte flow in an external magnetic field: A dimensionless analysis," *International Journal of Applied and Physical Sciences,* vol. 2, no. 1, pp. 13-20, 2016.
DOI: https://dx.doi.org/10.20469/ijaps.2.50003-1
To link to this article: http://kkgpublications.com/wp-content/uploads/2016/2/Volume2/IJAPS-50003-1.pdf

KKG PUBLICATIONS

International Journal of Applied and Physical Sciences

IJAPS

2016, 2(1): 13-20

ELECTROLYTE FLOW IN AN EXTERNAL MAGNETIC FIELD: A DIMENSIONLESS ANALYSIS

LANKA DINUSHKE WEERASIRI [1*], SUBRAT DAS [2]

[1, 2] Deakin University, Australia

Keywords:
Dimensionless Analysis
Lorentz Force
Bubble Induced Flow
Magneto-Hydrodynamics
Electrochemical Cell

Received: 10 November 2015
Accepted: 12 January 2016
Published: 16 March 2016

Abstract. In this paper, some recent work on the flow induced by an external magnetic field acting on an electrochemical cell is reviewed. Although the influence of the magnetic field on hydrodynamics has been studied for over five decades, magneto-hydrodynamics (MHD) remain relatively unfamiliar to all but a few research groups. Different authors have introduced nearly countless dimensionless parameters in electrolytic flow (bubble induced flow) and MHD, but they have been introduced for convenience. The similitude parameter proposed by [1] and [2] has been modified to provide a full set of parameters for electrolytic cells operating under an external magnetic field. The bubble sliding characteristics underneath an inclined plane are studied using copper sulfate solution (as an electrolyte) in a lab-based-scale and discussed.

INTRODUCTION

The phenomenon of the nucleation of bubbles under an inclined wall has crucial importance in a number of engineering applications such as cooling of nuclear reactor, top submergence of gas injection into molten metal, heat recovery in metallurgical process and numerous pharmaceutical processes [3]. In certain industrial applications such as the Hall–Héroult process, bubbles are nucleated primarily underneath surfaces. Bubble-induced flow in aluminium reduction cell is a complex phenomenon due to a number of factors such as electromagnetic forces (EMFs), surface tension, buoyant field, current density, voltage fluctuations, convective forces, geometry of the anode and the electrolysis process [4]. Figure 1 shows an aluminium reduction cell where electricity traverses vertically through the anode, cryolite, molten metal pool, cathode and returned on the collector bars to the external bus [5].

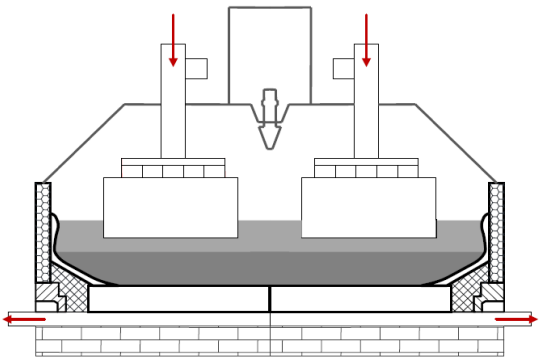

Fig. 1. Schematic representation of an aluminium reduction cell ([5], Figure 1)

Strong magnetic fields (B) are generated due to intense electrical current in the cathode bus bars. They interact with the current density vectors (J) in the conducting fluids to generate magneto-hydrodynamic (MHD) forces. According to [6], the source of instability in the metal is due to the vertical magnetic component (B_z) interacting with horizontal current density vectors.

The horizontal gradient of the vertical magnetic field should be limited to a minimum while interacting with the horizontal current [7]. These forces can have a significant influence on the side ledge and the surface of the cathode [8]; [16]. According to [8], the design of the inclined sidewall can have an impact on the MHD forces in metal pool. Stability in the metal pad can be achieved by either the magnetic compensation and/or improvising horizontal current (J) in the aluminium pool to further reduce the anode-cathode distance (ACD) [8].

The earliest study on the rise of bubbles underneath an inclined plane was the experimental studies reported by [9]. The experiments were conducted on a two-dimensional tank with deionized water and methanol which were used as the test fluids. Similarly, but a more comprehensive study on the characteristics of bubbles rising under inclined surface was conducted by [10]; [11]. Later, several studies [17]; [3] have reported the behaviour of bubbles underneath surfaces on lab-based physical models. [18] reported on the morphology and kinematics of Fortin bubbles with Particle Image Velocimetry (PIV) measurements and videography. Generally, the Reynolds (Re), Bond (Bo), Morton (Mo) and Froude (Fr) numbers are used to describe the morphology of the bubble, terminal velocity and the bulk bath

*Corresponding author: Lanka Dinushke Weerasiri
E-mail: lhweeras@deakin.edu.au

flow [12], [13], [14]. However, these laboratory-based physical models utilize a nozzle or a porous plate to generate bubbles, which in contrast to the Hall-Héroult process, forms bubbles electrolytically under intense magnetic field.

In recent times, renewed interest in the characteristics of electrolytically generated bubbles has risen. Nevertheless, the currently available research on the electrolytically generated bubbles from aluminium smelting point of view is meagre. [15] have recently reported that bubbles evolve in cluster underneath the electrode and that their coalescence process is enhanced by the presence of an external magnetic field.

Despite the recent development of laboratory-based electrolytic cells, the impact of magnetic fields, in terms of the Lorentz force induced in the electrolyte is yet undetermined. The Reynolds number, Eotvos number, Morton number and Froude number are not sufficient to explain the hydrodynamic characteristics of the cell when bubbles are electrolytically generated under an influence of an external magnetic field. This provides the motivation to carry out a dimensionless analysis considering all the variables including the external magnetic field for a typical Hall-Héroult cell. The goal is to provide a systematic approach to derive the dimensionless parameter using both Buckingham pi theorem and also by scaling the governing transport equation of momentum and mass.

DIMENSIONAL ANALYSIS AND THE PHYSICAL MODEL

The dimensionless numbers have certain advantages, they are independent of the system of units. These parameters apply to all physically similar systems, so they are useful for scale up/down. The schematic of the physical model that was used in this study is shown in Fig. 1. The tank is made of Perspex with dimensions of 300 x 150mm and 173mm height. An aqueous Copper (II) Sulphate ($CuSO_4$) solution with 0.5 Molarity was used as the electrolyte with a steel anode and a copper cathode. The materials of the anode and cathode avoid the generation of bubbles on the cathode. The Anode is held with a block that is machined to hold the anode at certain inclinations (0^o, 1^o and 2^o). To focus the bubble generation under the anode, the anode is coated with an insulating layer on all surfaces except the lower surface of the anode. An insulating barrier is also placed between the electrodes to restrict the flow of formed copper from the cathode towards the anode. This barrier will ensure the view of the nucleating bubbles underneath the anode is clear and uninterfered. The external static magnetic field is generated by placing a neodymium-based magnet next to the cell with a surface field of 1.8 Tesla. The aqueous Copper (II) Sulphate solution is broken down into Sulphuric acid, copper deposit and oxygen gas.

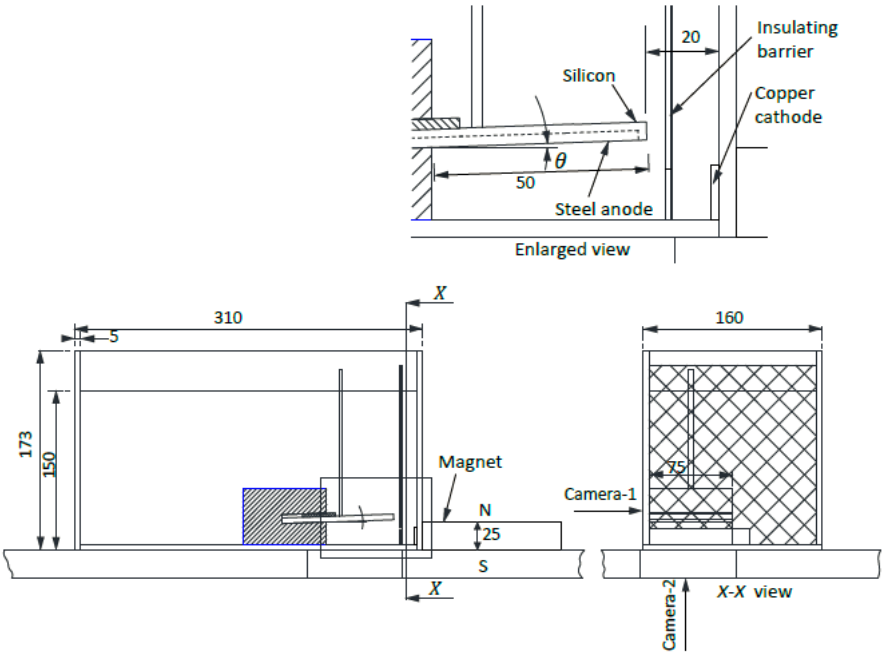

Fig. 1. Schematic represeantation of the cold-model lab-based electolytic cell

We consider the flow of an electrically conducting fluid, which is an aqueous Copper (II) Sulphate ($CuSO_4$) solution in an rectangular tank. The fluid is characterized by its electrical conductivity (σ), density (ρ), and the dynamic viscosity (μ). The flow characteristics in the physical model have been mainly focused on the motion set up by MHD induced flow field. The velocity gradients in the electrolyte are often measured to confirm the presence of Lorentz force. The bubbles indirectly experience the effects of the MHD forces through changes in the surrounding fluid's pressure, viscosity, density, surface tension and gravity

field. The number of variables that influence the flow characteristics of the bubbles that are generated electrolytically can be expressed as [15]:

$$v_b = f(\rho, \rho_b, \mu, L, d_b, \gamma, g, B, \sigma, Q, V)$$

The ρ and ρ_b are the density of the electrolyte and the density of the gas, respectively; μ is the dynamic viscosity of the electrolyte; γ is the surface tension and g is the gravity; B is the magnetic field; σ is the conductivity; Q and V are the gas formation rate [1] and bulk velocity of the electrolyte respectively; d_b is the diameter of the bubble and L is the characteristic length of anode.

The Buckingham PI theorem is used to develop the correlations representing flow characteristic caused by the nucleating bubbles. This method is selected for analysis since it allows the generation of all key dimensionless groups which characterize the problem even if the general form of the equation to be developed is unknown. It is to be noted that although mass transfer is dependent on temperature, the temperature effects are not included in this work since all experiments were performed at isothermal conditions.

The function f, given in equation 1, contains 12 dimensionally homogeneous variables (I=12), with four reference variables (j). According to the Buckingham Pi (π) theorem [24] this dictates that the number of independent dimensionless parameters needed to fully describe the behaviour of this system is 8. The number of repeating variables (ρ, μ, B and L) equals to the number of the reference dimensions (j = 4). These repeating variables are combined with the remaining variables to create following Pi groups.

$$\begin{array}{ll} \pi_1 = \rho^a \mu^b B^c d_b^d \rho_b & \pi_2 = \rho^a \mu^b B^c d_b^d L \\ \pi_3 = \rho^a \mu^b B^c d_b^d \gamma & \pi_4 = \rho^a \mu^b B^c d_b^d g \\ \pi_5 = \rho^a \mu^b B^c d_b^d \sigma & \pi_6 = \rho^a \mu^b B^c d_b^d Q \\ \pi_7 = \rho^a \mu^b B^c d_b^d V & \pi_8 = \rho^a \mu^b B^c d_b^d v_b \end{array} \qquad (2)$$

Dimensions of physical quantities are expressed as a product of the basic physical dimensions of mass (M), length (L), time (T) and ampere (A), such that the dimensions of the velocity are length/time (L/T or LT^{-1}). A summary of the variables with the dimensions can be given as follows:

TABLE 1
VARIABLES WITH THE BASIC PHYSICAL DIMENSIONS

Factors affecting bubble velocity	Units	MLTA
Density of the liquid (ρ)	$\frac{\mathrm{kg}}{\mathrm{m}^3}$	ML^{-3}
Density of the gas (ρ_b)	$\frac{\mathrm{kg}}{\mathrm{m}^3}$	ML^{-3}
Dynamic viscosity of the liquid (μ)	$\frac{\mathrm{kg}}{\mathrm{s} \cdot \mathrm{m}}$	$\mathrm{MT}^{-1}\mathrm{L}^{-1}$
Characteristic length of the anode (L)	m	L
Bubble diameter (d_b)	m	L
Surface tension of the liquid (γ)	$\frac{\mathrm{N}}{\mathrm{m}}$	MT^{-2}
Acceleration due to gravity (g)	$\frac{\mathrm{m}}{\mathrm{s}^2}$	LT^{-2}
Magnetic field (B)	$\frac{\mathrm{N}}{\mathrm{A} \cdot \mathrm{m}}$	$\mathrm{MT}^{-2}\mathrm{A}^{-1}$
Conductivity (σ)	$\frac{\mathrm{A}^2 \cdot \mathrm{s}^3}{\mathrm{kg} \cdot \mathrm{m}^3}$	$\mathrm{A}^2\mathrm{T}^3\mathrm{L}^{-3}\mathrm{M}^{-1}$
Gas formation rate (Q)	$\frac{\mathrm{m}^3}{\mathrm{s}}$	$\mathrm{L}^3\mathrm{T}^{-1}$
Bulk velocity of the electrolyte (V)	$\frac{\mathrm{m}}{\mathrm{s}}$	LT^{-1}

The exponents a, b, c and d are obtained from equation 2 with the requirement that πs are dimensionless, which lead to the following set of dimensionless parameters.

$$\frac{\rho v_b d_b}{\mu} = f\left(\frac{\rho}{\rho_b}, \frac{L}{d_b}, \frac{\rho d_b \gamma}{\mu^2}, \frac{\rho^2 d_b^3 g}{\mu^2}, \frac{\sigma B^2 d_b^2}{\mu}, \frac{\rho Q}{\mu d_b}, \frac{\rho V d_b}{\mu}\right) \quad 3$$

The above equation clearly illustrates that the bubble induced flow in electrolytic cell can be expressed as function of the Hartmann number (Ha) and the Stuart number (N), which can be written as [19]:

$$Ha^2 = \frac{\sigma B^2 d_b^2}{\mu} \quad 4$$

$$N = \frac{\sigma B^2 L}{\rho V} = \frac{Ha^2}{Re} \quad 5$$

The flow governed by a balance between inertia forces, pressure forces, viscous forces and Lorentz forces can be expressed in terms of conservation laws. The current density (j) in the Lorentz force term ($F = j \times B$) is determined by the gradient of the electric potential and the induced electric field due to the motion of the conducting electrolyte. The dimensional analysis of this governing equation also leads to two main non-dimensional parameters as Hartmann number and the Stuart number [20].

RESULTS AND DISCUSSION

We had previously demonstrated [15] that the MHD forces induced by a DC magnetic field affected the velocity and tracked displacement of the electrolytic bubbles in two cases of anode inclination (shown in figure 3). The velocity of the bubbles that was tracked using Image J with an Object tracking add-on showed that both cases of anode inclination were significantly affected by the MHD forces generated when a DC magnetic field was introduced to the experiment. The Velocity vs Displacement plots shown in figure 3 clearly demonstrate the magnitude of velocity and displacement affected on the tracked bubbles.

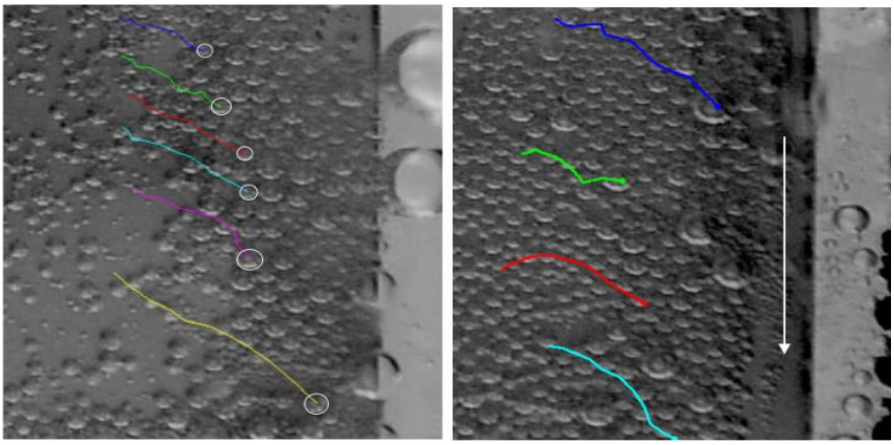

(a) (b)

Fig. 3. Bubble path lines from 16s to 27s (a) No magnetic field (b) with magnetic field [15]

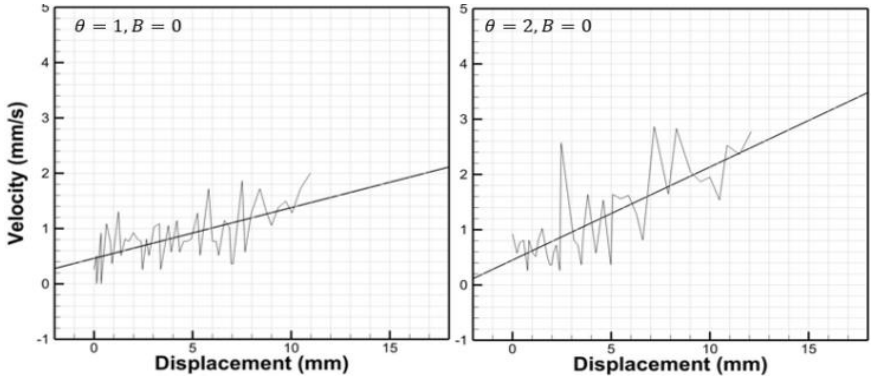

(a)

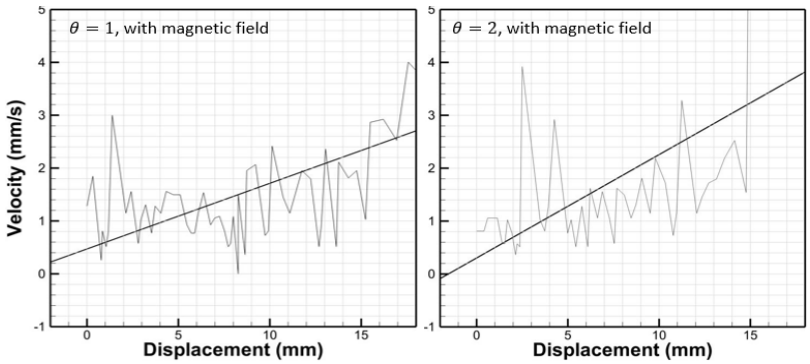

(b)

Fig. 4. Velocity data of a tracked bubble (a) no magnetic field (b) with magnetic field [15]

The vigorous fluctuation of velocity can be seen on all velocity plots. This is primarily due to the interaction of the tracked bubble with other bubbles that results in dynamic coalescence. Nevertheless, the straight-line plot that is superimposed on the velocity plots clearly demonstrates the trend of the velocity data in each case. It can be seen that the velocity of the experiments with the external magnetic field induces greater velocity, independent of the anode inclination. The Figure 4 also shows a complex velocity pattern due to coalescence process arising from bubble-bubble interaction. However, it is to be noted that due to the large number bubble nucleation on the anode surface at any instant of time makes it difficult to observe the growth of any particular bubble.

Thus, the experimental rig is modified in order to allow a single bubble to slide under similar electric and magnetic field. This is achieved by using copper anode and a copper cathode, which prevent the generation of gas bubbles at the anode while retaining the same electric and magnetic field throughout the cell. A single bubble can then be injected through an orifice at a controlled flow rate to study the impact of external magnetic field. The orifice diameter of 3mm is used for an inclined anode with an inclination of 8º. Images are taken using a high speed camera at 200 frames per second. A glass diffuser is also used in to obtain an even light sheet so that the camera can acquire a good contrast image of the bubble. The bubble path was tracked with ImageJ from its nucleation point at the orifice until it escaped from the side channel of the anode. The figure (a) shows the traversing of bubble in a linear path without the influence of an external magnetic field, which is consistent with normal bubble behaviour. However, under the influence of external magnetic field it can be seen that bubble path is skewed towards the right (seen in figure (b)). Although it is expected that the magnetic field will have some impact on conducting fluid but such a large deviation from the centre line is rather surprising, as it implies the dominance of EMF induced flow rather than only a bubble induced flow. It is to be noted that the electrolytically generated bubbles underneath the anode surface show more complex hydrodynamics when compared with a single injected bubble. This is mainly attributed to the rate of growth and the size of the bubble and thus the dominance of gravity field (buoyancy force) on the single injected bubble. Therefore, the order of magnitude of magnetic interaction with the given size of bubble may not be comparable. Nevertheless, the effect of the MHD induced flow field is significant throughout the cell.

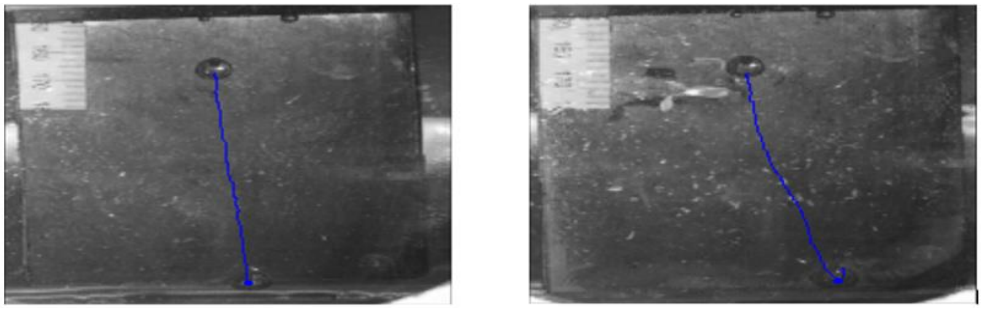

(a) (b)

Fig. 5. Bubble path from nucleation to release (a) without magnetic field (b) with magnetic field

To determine the effect of MHD parameter, the Hartmann number is calculated at three locations of the anode (D) 20, 40 & 60 mm from the external magnetic source. The strongest magnetic field with the highest concentration of current density is

expected at the end of the anode, which is 20mm from the magnetic source. The fluid properties that are required to calculate the Hartmann number are the conductivity at 6.23 s/m and dynamic viscosity of 0.917×10^{-3} Ns/m^2 [21].

The magnetic field strength at the three locations is determined from previously measured data from a gauss meter [15]. The equivalent bubble diameter (d_b) is calculated using the bubble base area (A) [22] using Image J analysis.

$$d_b = \sqrt{\frac{4}{\pi} A} \qquad 6$$

The Hartmann number for each location of the anode is calculated from the equation 4, which shows how strongly the hydrodynamics is influenced by the magnetic field [23]. It is observed that the Hartmann number reduces when the distance is greater from the source of magnetic field. Moreover, the current density is highest at the end of the anode, as it traverses in least resistance path that is the closest region of the anode to the cathode which further emphasizes that the electrolyte velocity field is more influenced when the magnetic field strength is higher.

TABLE 2
HARTMANN NUMBER FOR THREE LOCATIONS OF THE ANODE

D (mm)	B (Tesla)	A (mm^2)	d_b (m)	Ha
20	0.072	45.444	0.007606648	0.045142456
30	0.045	40.444	0.00717564	0.02661537
40	0.029	39.333	0.007076746	0.016915738
50	0.020	36.222	0.006791118	0.011195168
60	0.014	37.889	0.00694563	0.008014917

Plotting the data for the Hartmann number vs the Distance from the anode plot (shown in figure 6) revealed the gradual rise of Hartmann number, which indicates the gradual change in the influence of the Lorentz force in the flow field. However, as the flow field in the bath is a combination of the MHD induced and bubble induced flow field, the effect of the Lorentz force on the bubble has been shown not to be as gradual as the change in Hartmann number. This can be seen in the bubble path (shown in figure 6) that doesn't change gradually.

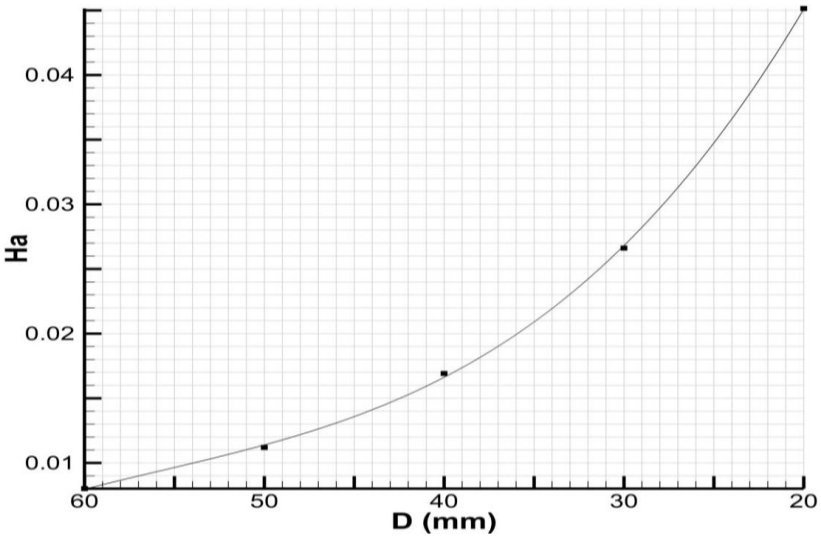

Fig. 6. Hartmann number vs distance from the magnet

Even though the bubble path was longer due to the magnetic field skewing the bubble path, the time that the bubble took to reach the end of the anode was 2 seconds less than bubble traversing without any external magnetic field. This is significant as the displacement of the bubble with the magnetic field was longer in comparison to the linear path of bubble without the MHD induced flow field.

The deviation of the bubble under the influence of the magnetic field from the vertical path is shown in figure 7. The X-axis deviation plot shows the scattering of data points indicating a gradual change, which is best seen with the general curve fit,

however, it is not as consistent as the trend of the Hartmann number vs Magnetic source distance plot (given in figure 7). As mentioned previously, the combined flow field may be a contributor to this inconsistency. The general curve fit illustrates a significant deviation from the centre line indicating the influence of the magnetic interaction parameter. A stiffer velocity gradient is observed from 30 to 32 seconds as the bubble moves towards the area of higher magnetic field. This leap is the highest change in x deviation, considering the average is approximately 1.08mm.

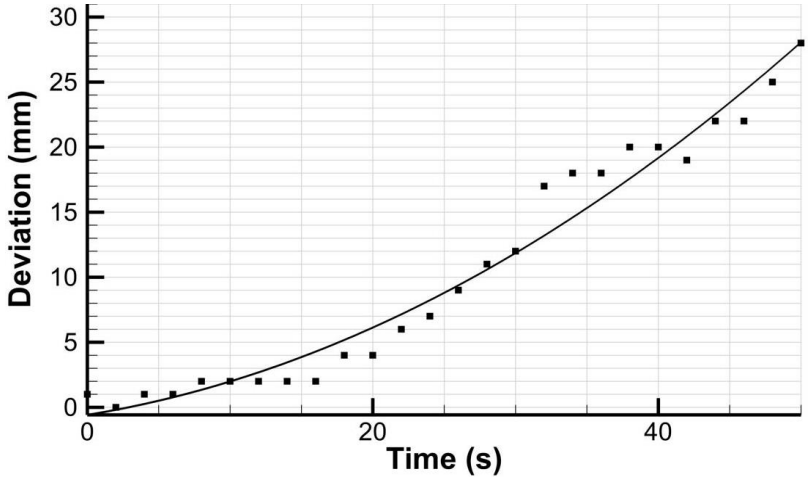

Fig. 7. X-axis deviation for bubble with magnetic field plot

CONCLUSION

The laboratory-based electrolytic cell is designed to achieve dynamic similarity between the scaled model and an industrial aluminium reduction cell to study the impact of EMF-induced flow. The impact of an external magnetic field on bubble underneath anode surface is analyzed. The primary forces found to be governing the overall bubble behaviour are the inertial forces derived from the flow and the buoyancy force of the bubble without the presence MHD forces.

It has been demonstrated that the superposition of a magnetic field during aqueous $CuSO_4$ electrolysis, regardless of the anode inclination, significantly affects the bubble velocity and its traversing path. In the future, we are planning to make Particle Image Velocimetry measurements to quantify the velocity field to relate the magnetic interaction parameter to bubble sliding velocity.

REFERENCES

[1] A. Solheim, S. T. Johansen, S. Rolseth and J. Thonstad, "Gas induced bath circulation in aluminium reduction cells," *Journal of Applied Electrochemistry*, vol. 19, no. 5, pp. 703-712, 1989.

[2] A. Perron, L. I. Kiss and S. Poncsák, "An experimental investigation of the motion of single bubbles under a slightly inclined surface," *International Journal of Multiphase Flow*, vol. 32, no. 5, pp. 606-622, 2006.

[3] S. Das, Y. S. Morsi, G. Brooks, J. J. J. Chen and W. Yang, "Principal characteristics of a bubble formation on a horizontal downward facing surface," *Colloids and Surfaces: A Physicochemical and Engineering Aspects*, vol. 411, pp. 94-104, 2012.

[4] S. Das, G. Littlefair, Y. Morsi and G. Brooks, "Tracking single bubble in hall-héroult aluminium cell: an experimental and numerical study," In ISTEC 2012: Proceedings of the 3rd International Science & Technology Conference, 2012.

[5] S. Das and G. Littlefair, *Current Distribution and Lorentz Field Modelling Using Cathode Designs: A Parametric Approach Light Metals 2012* (pp. 845-851): John Wiley & Sons, Inc, 2012.

[6] T. Sele, "Instabilities of the metal surface in electrolytic alumina reduction cells," *Metallurgical Transactions B*, vol. 8, no. 4, pp. 613-618, 1977.

[7] N. Urata, "Magnetics and metal pad instability," In Light Metals: Proceedings of Sessions, AIME Annual Meeting, Warrendale, Pennsylvania, 1985.

[8] S. Das, G. Brooks and Y. Morsi, "Theoretical investigation of the inclined sidewall design on magnetohydrodynamic (MHD) forces in an aluminum electrolytic cell," *Metallurgical and Materials Transactions B*, vol. 42, no. 1, pp. 243-253, 2011.

[9] C. C. Maneri and N. Zuber, "An experimental study of plane bubbles rising at inclination," *International Journal of Multiphase Flow*, vol. 1, no. 5, pp. 623-645, 1974.

[10] T. Maxworthy, "Bubble rise under an inclined plate," *Journal of Fluid Mechanics*, vol. 229, pp. 659-674, 1991.

[11] T. Maxworthy, C. Gnann, M. Kürten and F. Durst, "Experiments on the rise of air bubbles in clean viscous liquids," *Journal of Fluid Mechanics*, vol. 321, pp. 421-441, 1996.

[12] D. Bhaga and M. E. Weber, (1981). "Bubbles in viscous liquids: Shapes, wakes and velocities," *Journal of Fluid Mechanics*, vol. 105, pp. 61-85, 1981.
[13] J. Grace, T. Wairegi and T. Nguyen, "Shapes and velocities of single drops and bubbles moving freely through immiscible liquids," *Trans. Inst. Chem. Eng.*, vol. 54, no. 3, pp. 167-173, 1976.
[14] T. Maxworthy, "Experimental studies in magneto-fluid dynamics: Pressure distribution measurements around a sphere," *Journal of Fluid Mechanics*, vol. 31, no. 04, pp. 801-814, 1968.
[15] S. Das, L. D. Weerasiri and V. Jegatheesan, *Bubble Flow in a Static Magnetic Field Light Metals 2015* (pp. 789-793): John Wiley & Sons, Inc, 2015.
[16] M. Dupuis and V, Bojarevics, "Busbar sizing modeling tools: comparing an ANSYS® based 3D model with the versatile 1D model part of MHD-Valdis," *Light Metals*, pp. 341-346, 2006.
[17] J. J. J. Chen, Z. Jian Chao and Q. Kang Xing, "Rise velocity of air bubble under a slightly inclined plane submerged in water," In The Fifth Asian Congress of Fluid Mechanics, Taejon, Korea, 1992.
[18] A. Caboussat, L. Kiss, J. Rappaz, K. Vékony, A. Perron, S. Renaudier and O. Martin, *Large Gas Bubbles under the Anodes of Aluminum Electrolysis Cells. In S. J. Lindsay (Ed.), Light Metals 2011* (pp. 581-586): John Wiley & Sons, Inc, 2011.
[19] X. Miao, D. Lucas, Z. Ren, S. Eckert G. Gerbeth, "Numerical modeling of bubble-driven liquid metal flows with external static magnetic field," *International Journal of Multiphase Flow, 48*, 32-45, 2013.
[20] S. Das, "Convection in fluid overlying porous layer: an application to Hall-Heroult cell," *Materials Performance and Characterization*, vol. 1, no. 1, pp. 1-22, 2012.
[21] D. Price and W. Davenport, "Densities electrical conductivities and viscosities of CuSO4/H2SO4 solutions in the range of modern electrorefining and electrowinning electrolytes," *Metallurgical Transactions B*, vol. 11, no. 1, pp. 159-163, 1980.
[22] J. A. M. Kuipers, W. Prins and W. P. M. V. Swaaij, "Theoretical and experimental bubble formation at a single orifice in a two-dimensional gas-fluidized bed," *Chemical Engineering Science*, vol. 46, no. 11, pp. 2881-2894, 1991.
[23] C. Heinicke, S. Tympel, G. Pulugundla, I Rahneberg, T. Boeck and A. Thess, "Interaction of a small permanent magnet with a liquid metal duct flow," *Journal of Applied Physics*, vol. 112, no12, pp. 124-924, 2012.
[24] M. C. Ruzicka, "On dimensionless numbers," *Chemical Engineering Research and Design*, vol. 86, no. 8, pp. 835-868, 2008.

–This article does not have any appendix–